

Equatorial Entrainment Zone : the Diurnal Cycle

Roland W. GARWOOD, Jr¹, P.C. CHU¹, Peter MULLER² and Niklas SCHNEIDER²

¹ *Department of Oceanography, Naval Postgraduate School
Monterey, CA 93943 - U.S.A.*

² *Department of Oceanography, University of Hawaii at Manoa
Honolulu, HI 96822 - U.S.A.*

Abstract. A model for the entrainment zone of the equatorial turbulent boundary layer is used to compute the turbulent fluxes of buoyancy and momentum and the dissipation of turbulent kinetic energy in the pycnocline well below a relatively shallow (order 20 m) quasi-homogeneous surface layer. In the presence of a steady westward wind stress, diurnal variation of the surface buoyancy flux triggers dynamic instabilities that "ripple" downward (order 100 m) during the night into the pycnocline above the undercurrent core, causing a strong diurnal cycle in dissipation and in the depth of penetration of the turbulent fluxes into the upper 100-150 meters of the water column.

1. Introduction

It may seem that observations of the rate of dissipation of turbulent kinetic energy, $\epsilon(z)$, in the equatorial oceans have raised as many new questions as have been resolved. New investigations have been stimulated concerning the importance of the undercurrent shear (Crawford and Osborn, 1981), sampling biases and the relative importance of spacial (meridional) and temporal (diurnal) structures to the dissipation field (Moum *et al.*, 1986), the relationship between dissipation and eddy mixing coefficients (Peters *et al.*, 1988), and the computation of Reynolds stress with dissipation-method techniques accepted in non-equatorial domains (Dillon *et al.*, 1989).

Although an overall understanding of the dynamics of equatorial turbulence has not yet emerged, consistent descriptions of the diurnal cycle of dissipation on the equator have been documented (Paka and Fedorov, 1982; Peters *et al.*, 1988; and Moum *et al.*, 1989). However, none of the mixed layer model applications at the equator to date (including Hughes, 1980; Schopf and Cane, 1983; and Garwood *et al.*, 1985) appear to have adequate physics to explain the deep diurnal penetration of dissipation below the well-mixed surface layer. Although Garwood *et al.* (1985) showed that the northward component of planetary rotation may act with the Reynolds stress to increase the depth of the well-mixed layer, this mechanism cannot explain the diurnal increase of dissipation in the pycnocline well below the surface layer.

The scientific objective of a collaborative equatorial mixed layer study by the Departments of Oceanography at the Naval Postgraduate School and the University of Hawaii is to understand and construct models for the dynamics and thermodynamics of the equatorial and tropical mixed layer system. Here we report model results that offer an explanation for how turbulence that is locally generated by surface forcing can "penetrate" rapidly and deeply into the not-so-well-mixed zone between the surface well-mixed layer and the undercurrent core. The Naval Postgraduate School mixed layer model (Garwood, 1977) is augmented to include a finite-thickness entrainment zone that was postulated for possible general application



F 30230

at all latitudes (Garwood, 1987), but has been neglected at the equator. The equatorial mixed layer system appears to be an ideal location to verify this phenomenon because of the strong vertical shear, the lack of rotation and the nearly steady surface wind.

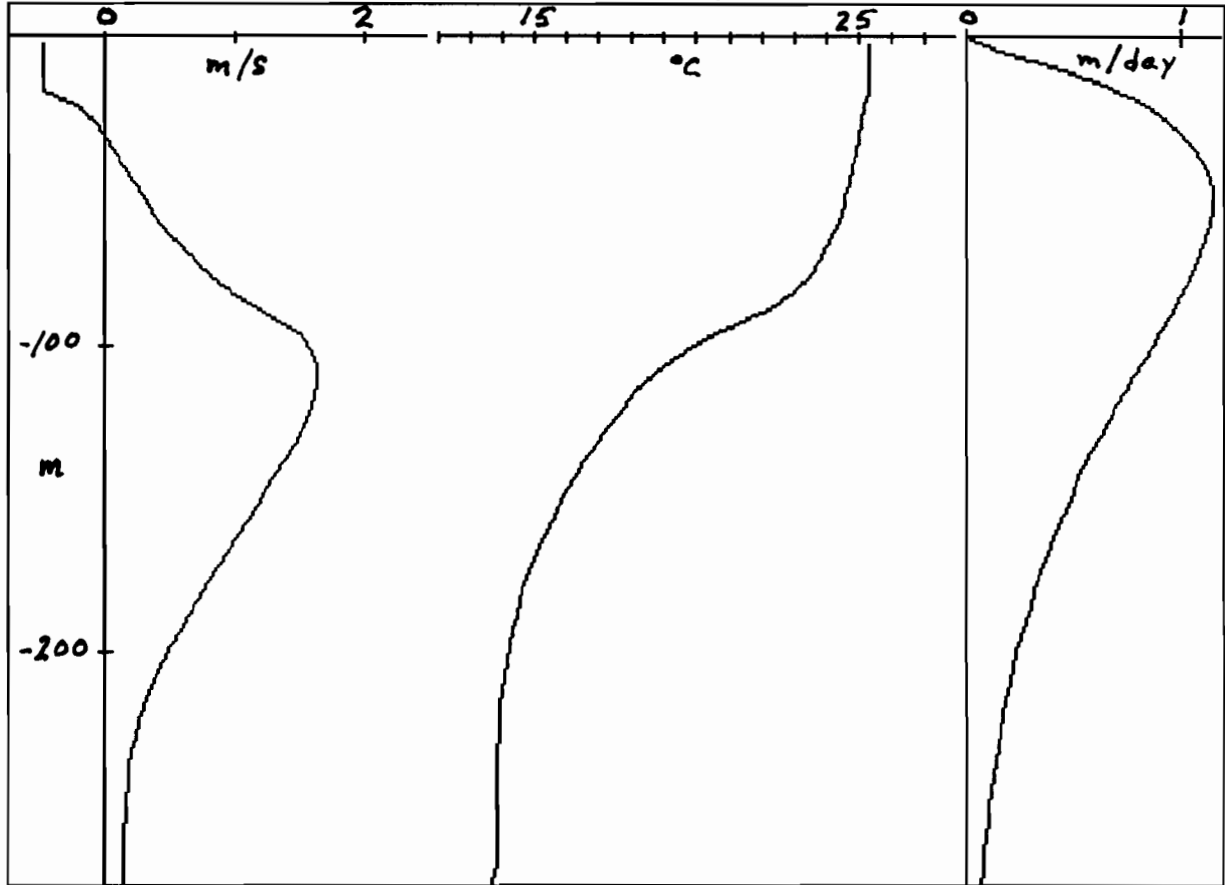


Figure 1 Steady-state model solutions for (a) zonal velocity $U(z)$ and (b) temperature $T(z)$ using prescribed (c) vertical velocity $W(z)$, and constant surface wind stress and constant heating.

2. Steady-State Finite-Thickness Entrainment Zone With Upwelling

The mixing model for the entrainment zone is based upon two hypotheses. Firstly, there will be no significant turbulent fluxes of mass, momentum or buoyancy unless the gradient Richardson number is less or equal to a critical value, $Ri \leq Ri_{CR} \sim \frac{1}{4}$. Secondly, if a dynamic instability is initiated, the mixing ratios of momentum and buoyancy will be equal and just sufficient to achieve dynamic stability. This method has been established by Adamec *et al.* (1981), but has not been applied previously to flows at the equator. The value of Ri_{CR} that is appropriate for the entrainment zone at the equator appears to be about $\frac{1}{4}$ or somewhat larger (Gregg *et al.*, 1985 and Peters *et al.*, 1988). Possibly, Ri_{CR} should not even be constant in time. If internal wave energy is propagated vertically (Muller, 1976) in the entrainment zone, it is possible that the vertical convergence of pressure transport of turbulent kinetic energy contributes significantly to the turbulent kinetic energy budget in the entrainment zone (Dillon *et al.*, 1989). This extra source of energy would cause the value of Ri_{CR} to be greater than the commonly assumed value of $\frac{1}{4}$. A range of values up to $\frac{1}{2}$ have been tested, but the results shown here were all derived with the traditional value of $Ri_{CR} = \frac{1}{4}$.

Implicit in the application of this entrainment model is the assumption that the entrainment zone is marginally dynamically stable. A slight decrease in the downward buoyancy flux at the top of the entrainment zone will trigger a dynamic instability that may "ripple" down a considerable distance until it reaches a part of the water column that is sufficiently stable to stop the vertical propagation of the event.

Figures 1 (a) and (b) show profiles of the mean zonal velocity and the temperature that are generated by spinning up the mixed layer-entrainment model to an approximate steady state under the conditions of a time-invariant wind stress, a diurnally varying surface buoyancy (heat) flux, a prescribed vertical velocity (Figure 1 c) and a prescribed zonal pressure gradient (not shown) that decays exponentially in depth (Dillon *et al.*, 1989) with a zonal surface slope, $\eta_x = -0.5 \times 10^{-7}$. For this case the net downward surface heat flux is taken to be $Q_0 = 100$ watts/m². The wind stress is westward, $\tau_x = -10^{-4}$ Nm⁻² and $\tau_y = 0$.

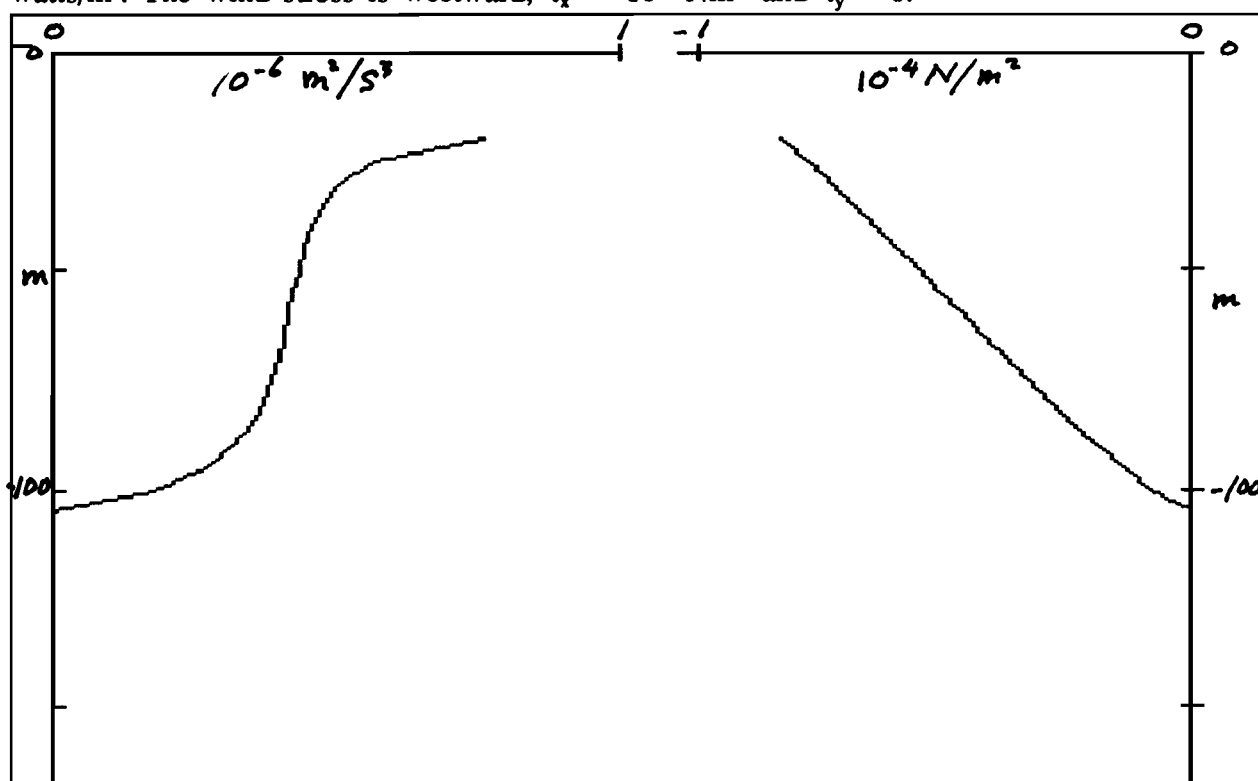


Figure 2 (a) Dissipation and (b) Reynolds' stress profiles for constant surface forcing case.

With no surface buoyancy flux, at mid latitudes planetary rotation would limit the depth of penetration of momentum and kinetic energy from the wind to Rossby and Montgomery's (1935) neutral planetary boundary layer scale $\sim u_* / f$, where u_* is the surface friction velocity and f is the Coriolis parameter. This also appears to be the scale size of the potential maximum thickness of the "entrainment zone" below a shallowing mixed layer that is surface-heated and wind-stirred (Garwood, 1987). Under the influence of a net downward surface buoyancy flux $B_0 > 0$, the thickness of the surface well-mixed layer above the entrainment zone is expected (Muller *et al.*, 1984) to be proportional to be equal to one half the Obukhov length scale, $h = L/2 \approx u_*^3 B_0^{-1}$ (Obukhov, 1946), and the underlying entrainment zone reaches a maximum thickness of approximately $0.2 u_* / f$. At higher latitudes, the entrainment zone has typically been approximated as a discontinuity. As $f \rightarrow 0$, the entrainment zone would thicken indefinitely were it not for advection. At the equator, in the absence of rotation, a mean upwelling velocity

$W > 0$ enables a steady state in the entrainment zone of thickness $\delta \sim 100$ m beneath the well-mixed surface layer of depth $h \sim 20$ m. Figure 2 shows that the dissipation and the Reynolds stress terminate at a depth of about 110 m, well below the well-mixed layer.

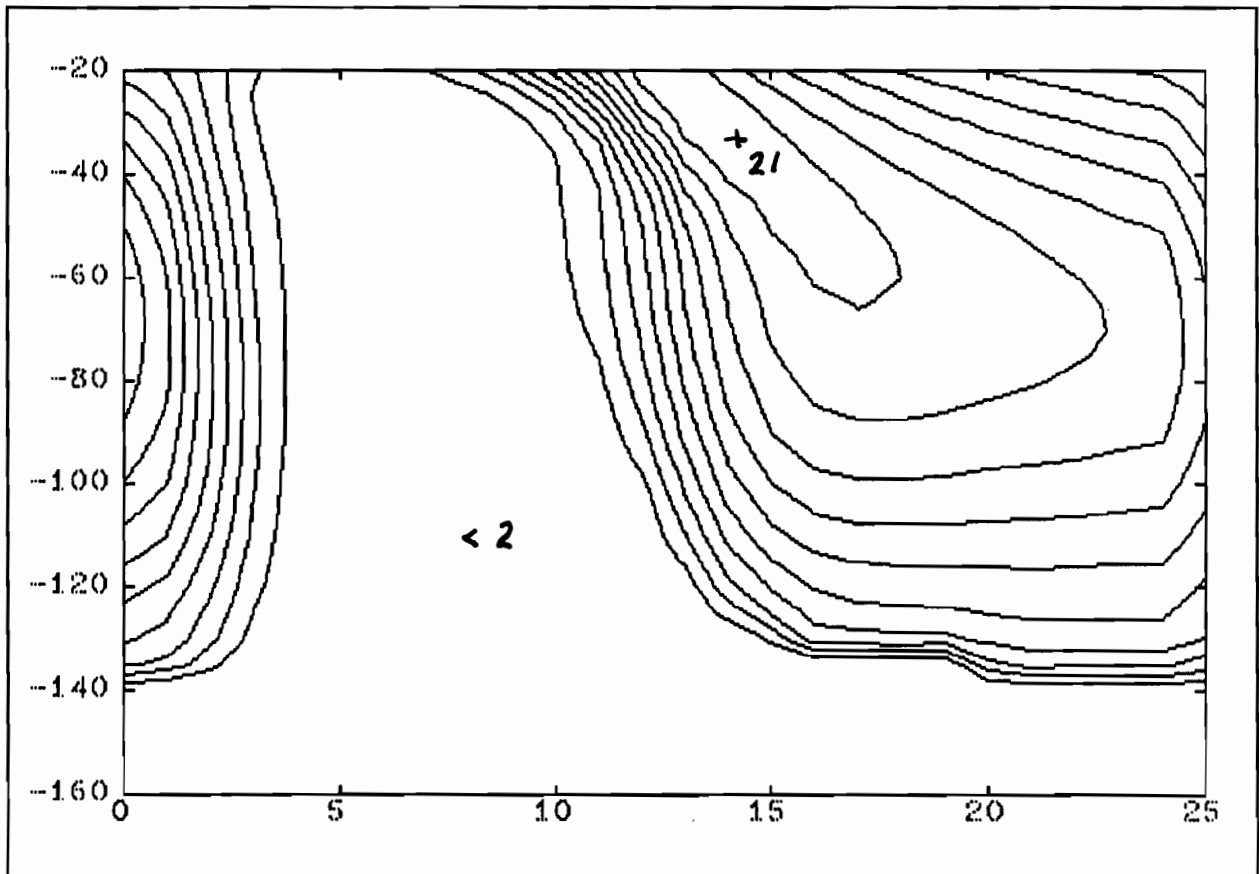


Figure 3 Contours of $\epsilon(t, z)$ at interval of $2 \times 10^7 \text{ m}^2 \text{ s}^{-3}$. Time is hours after local sunrise, and depth is meters below surface.

3. Response to Diurnal Surface Buoyancy Flux and Constant Wind Stress

After the model has come to an approximate steady-state condition, with the profiles of velocity, temperature, dissipation and stress shown in Figures 1 and 2, the surface heat flux is changed to include an incident solar radiation having a maximum value of 800 watts/m^2 at noon. The total heat flux plus radiation is adjusted so that the daily-average net heat input at the surface is still 100 watts/m^2 .

Although the values of the surface fluxes, averaged over one day, are unchanged, the modeled mixed layer-entrainment zone system requires a few days to again achieve a near equilibrium state. Four days after initiating the diurnally-varying surface heat flux, a cyclical steady state is achieved approximately. The diurnal response of the dissipation (Figure 3) shows that the dissipation of turbulent kinetic energy below the mixed layer falls to near zero from about 3 hours after sunrise until almost sunset. At the top of the entrainment zone, $z = -20$ m, the maximum dissipation rate of $2.1 \times 10^7 \text{ m}^2 \text{ s}^{-3}$ occurs at about hour 13 (7 p.m. local time). The time of maximum dissipation is depth dependent. The time of maximum

dissipation occurs later and later with depth. The peak dissipation at $z=-120$ m does not occur until just before sunrise.

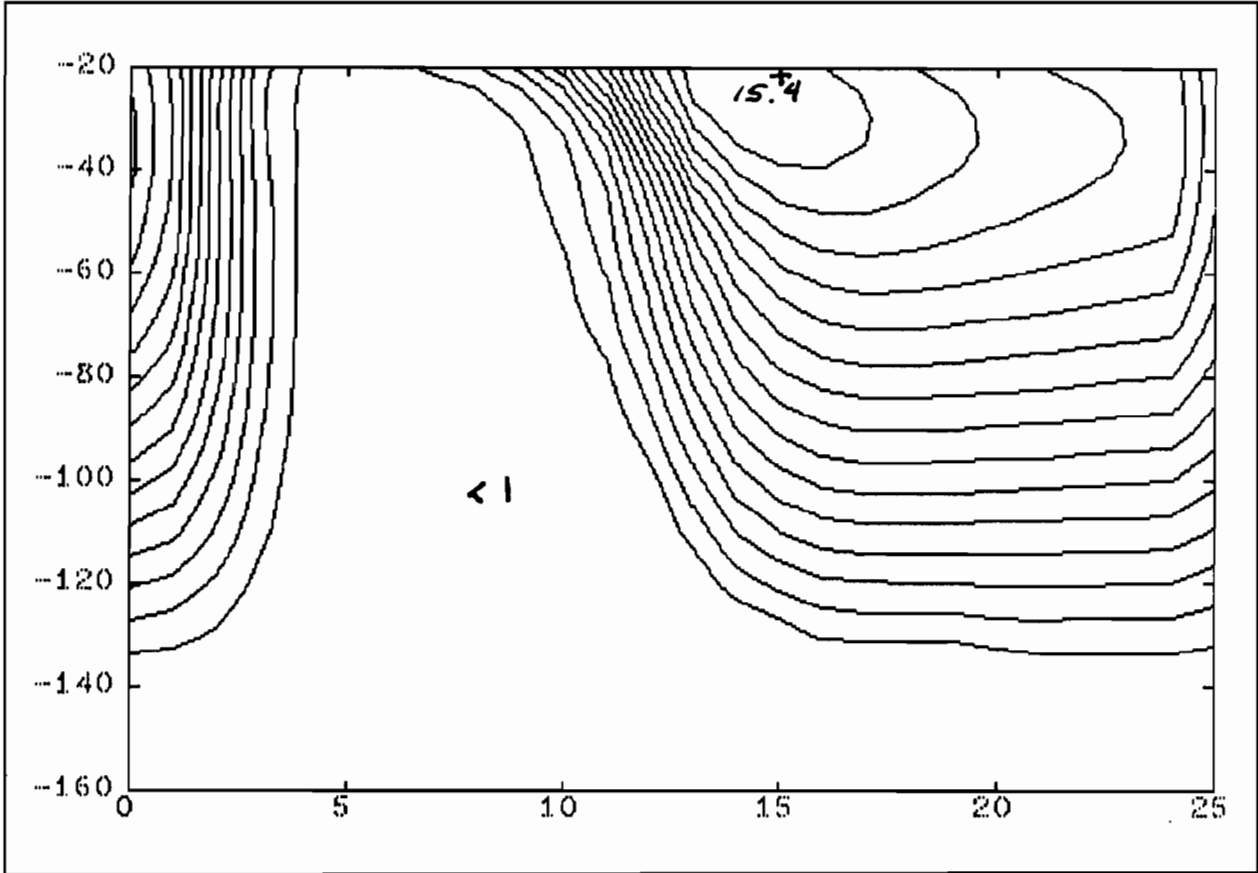


Figure 4 Contours of $uw(t,z)$ at an interval of $10^5 \text{ m}^2\text{s}^{-3}$.

The structures of the vertical fluxes of momentum (Figure 4) and heat (Figure 7) also have a strongly diurnal behavior. With the diurnal variation in the prescribed net heat flux, the diurnal dependence for the turbulent heat flux is not surprising. However, the maximum downward heat flux (exceeding 400 watts/m^2) at $z=-100$ m doesn't occur until about 14 hours after local noon (hour 20). The vertical dependence of the zonal stress also has a strong diurnal dependence, even though the surface stress is held constant at 10^4 Nm^2 . It is noteworthy, also, that the maximum stress near the top of the entrainment zone at $z\approx-30$ m exceeds the surface stress by more than 50%. This phenomenon is explained by the daytime storage of momentum in the overlying well-mixed layer. This momentum is released to the re-activated entrainment zone by the dynamic instability that starts in the late afternoon and continues throughout the night.

In spite of the large diurnal variation in the fluxes, the value of the gradient Richardson number changes only slightly in the region between $z=-30$ m and $z=-120$ m (Figure 5). In the turbulently inactive region, Ri increases because of net effects of vertical advection and the baroclinic component of the horizontal pressure gradient. If it weren't for advection and the horizontal pressure gradient, the value of Ri would be identically equal to the critical value for this model solution.

The results of these solutions here suggest that the intensity of turbulence and mixing in the entrainment zone does not depend upon the gradient Richardson number, to a first order. To demonstrate this point, the effective vertical eddy viscosity, $K_M = -uw(\partial U/\partial z)^{-1}$, was

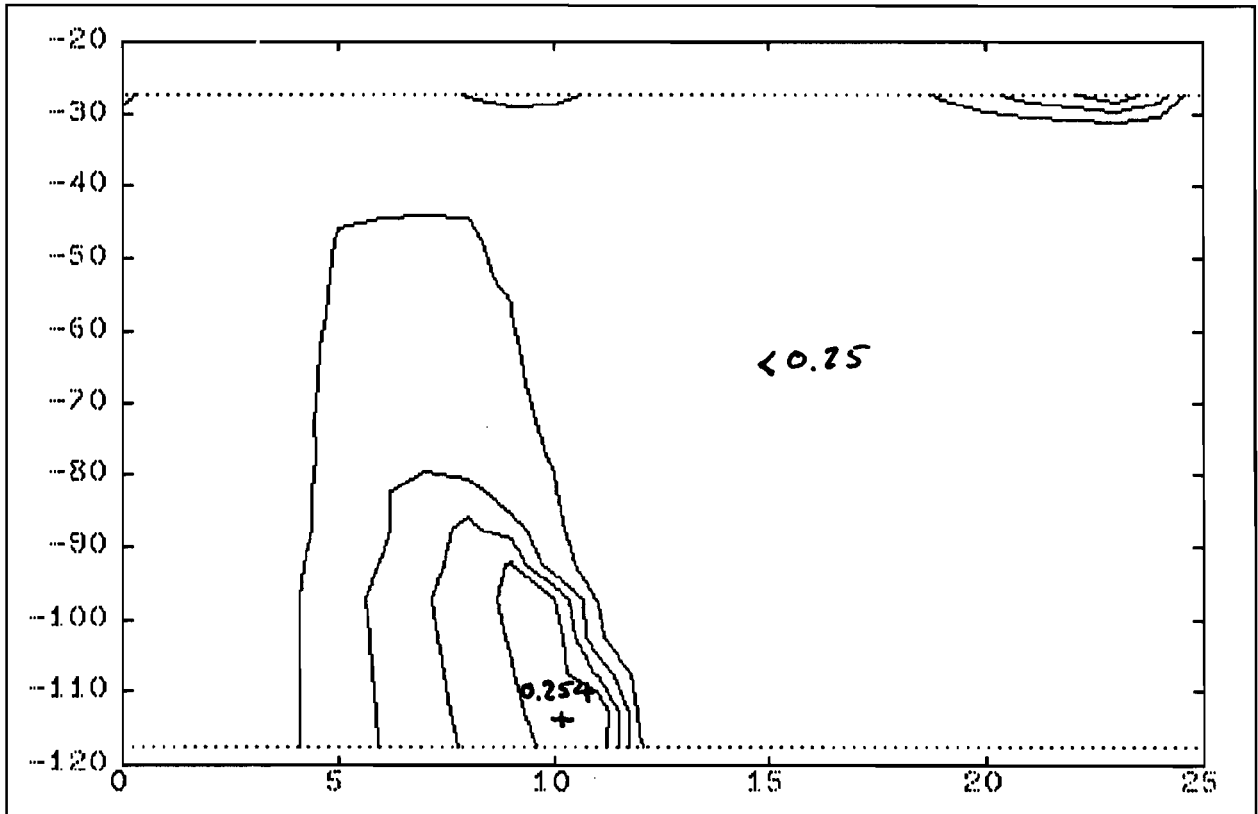


Figure 5 Contours of $Ri(z,t)$ at interval of 10^{-3} .

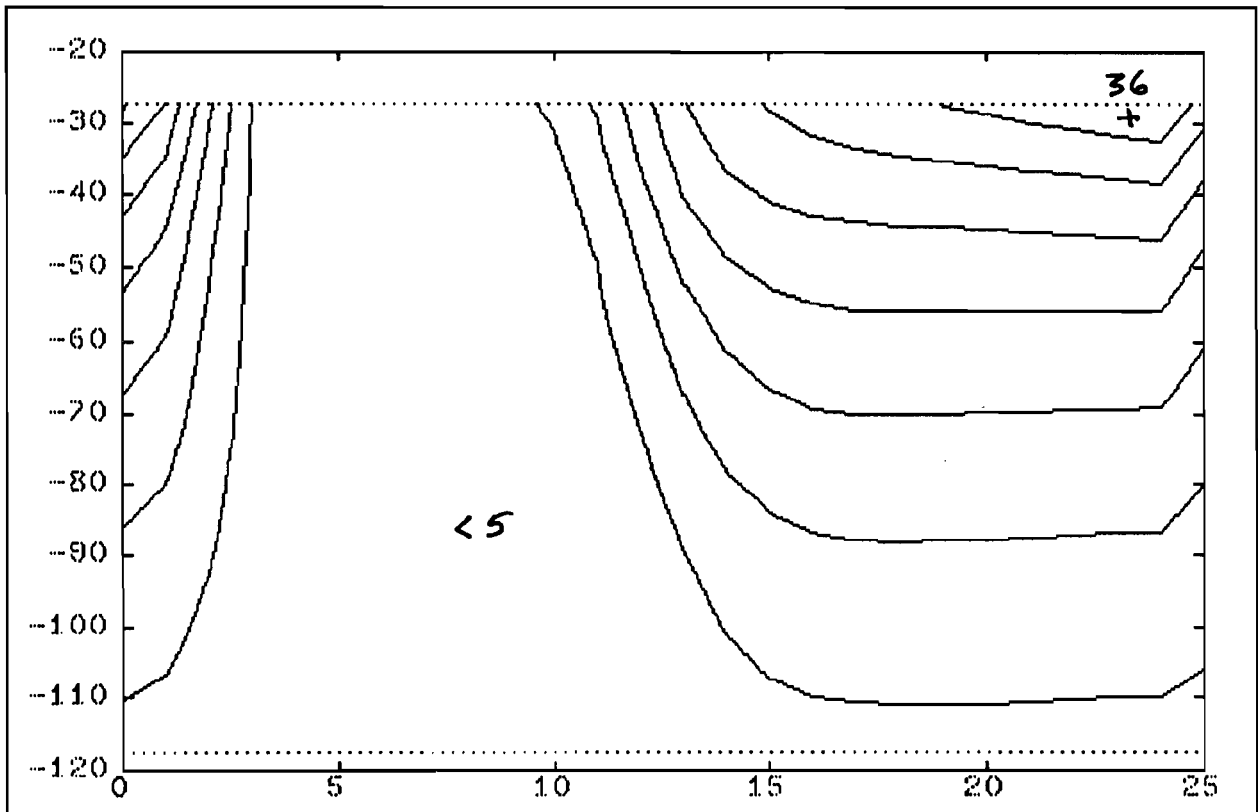


Figure 6 Contours of K_M at interval of $5 \times 10^{-3} \text{ m}^2 \text{ s}^{-1}$.

computed (Figure 6). As can be seen K_M varies between 0 and more than $30 \times 10^{-3} \text{ m}^2 \text{ s}^{-1}$, while Ri is nearly constant. This result supports the conclusion of Peters *et al.* (1988) that earlier models for $K_M(Ri)$ are inadequate for application at the equator.

4. Conclusions

Although the equatorial momentum budget is still not well understood, realistic vertical profiles for the zonal velocity and the temperature are predicted by application of typical values of local surface forcing, the pressure field, and the vertical velocity, together with the proposed mixed layer-entrainment model. Vertical mixing adjusts on a several-day time scale to cause a near equilibrium balance between advection and vertical mixing.

Entrainment mixing is modulated strongly at depths well below the relatively shallow well-mixed surface layer by the diurnal cycle in the surface buoyancy flux. Instabilities initiated just below the surface layer ripple down into the water column and reach the deepest extent only after many hours. This causes a considerable phase delay in dissipation and in the turbulent fluxes, relative to the phase of the surface buoyancy flux.

This study needs to be widened to address several questions:

- i) What is the appropriate value for the critical Richardson number at the equator, and is this really a universal constant for all oceanic entrainment zones?
- ii) What is the effect of transient wind events, with changes in both speed and direction? To address this second question, the prognostic model needs to be made fully three-dimensional, with model-computed advection instead of prescribing the non-local terms of the momentum budget, as done for this initial simulation.
- iii) Does this dynamic instability process influence the region below the undercurrent, also a high-shear zone? Numerical experimentation indicates that this region may become dynamically unstable, depending upon the vertical velocity field and the baroclinicity of the flow. Turbulence beneath the undercurrent does not appear to be as strong in this region, however, as it is above the undercurrent core.
- iv) What is the role of asymmetry about the equator in the surface forcing? Meridional fluxes may be significant, and even transient meridional velocity events they may have an important role in determining the equilibrium state at the equator.

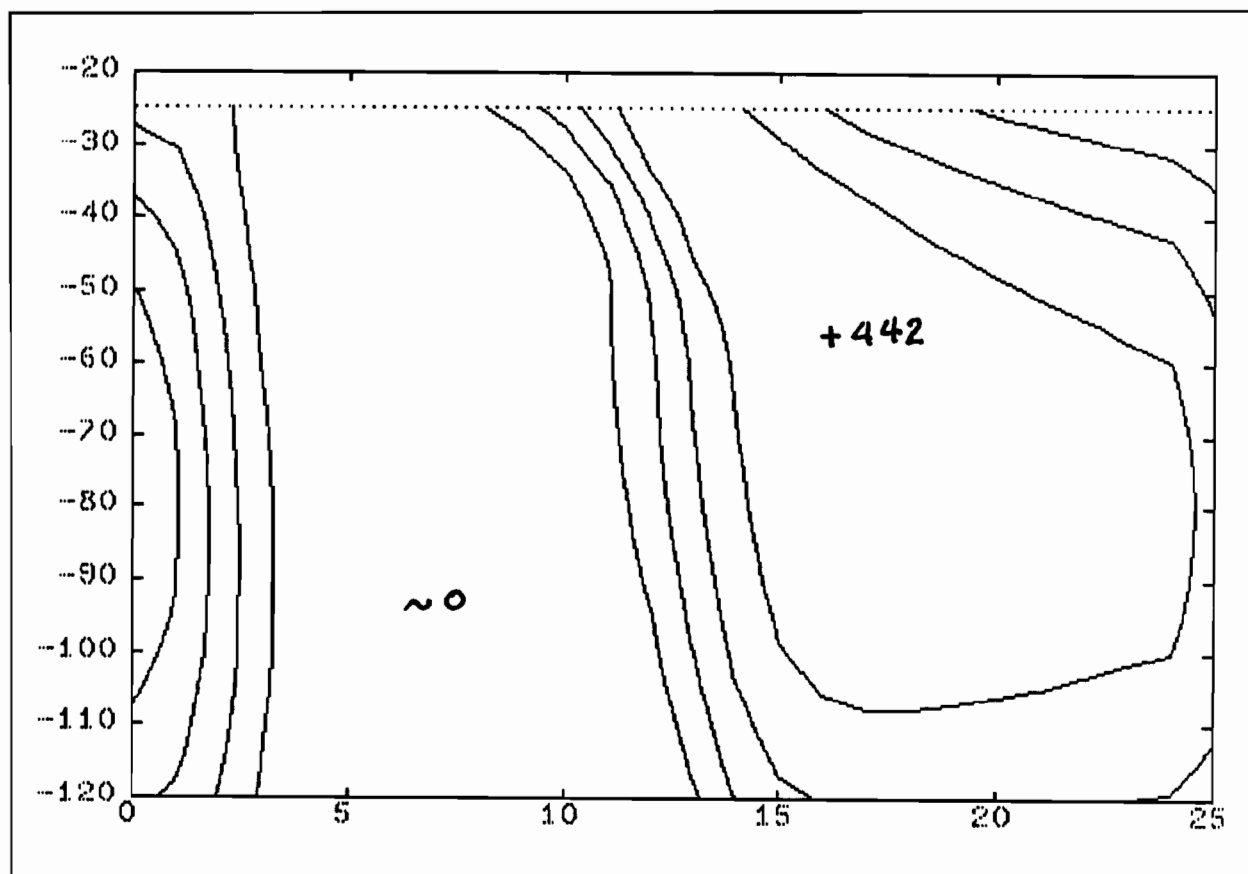


Figure 7 Contours of $-pc,T'w'$ at interval of 100 watts/m².

References

Adamec, D. D., R. L. Elsberry, R. W. Garwood, Jr., and R. L. Haney, 1981: An embedded mixed layer ocean circulation model. *Dyn. Atmos. Oceans*, **6**, 69-96.

Bryden, H. L., and E. C. Brady, 1985: Diagnostic model of the three-dimensional circulation in the upper equatorial Pacific Ocean. *J. Phys. Oceanogr.*, **15**, 1255-1273.

Crawford, W. R., and T. R. Osborn, 1981: Control of equatorial ocean currents by turbulent dissipation. *Science*, **212**, 439-540.

Dillon, T. M., J. N. Moum, T. K. Chereskin, and D. R. Caldwell, 1989: Zonal momentum balance at the equator. *J. Phys. Oceanogr.*, **19**, 561- 570.

Garwood, R. W., Jr., 1977: An oceanic mixed layer model capable of simulating cyclic states. *J. Phys. Oceanogr.*, **7**, 455-468.

Garwood, R. W., Jr., 1987: Unsteady shallowing mixed layer. *Proceedings 'Aha Huliko'a*, Hawaiian Winter Workshop, January 1987, Hawaii Inst. of Geophys. Special Publication, P. Muller and D. Henderson, Eds., 119-129.

- Garwood, R. W., Jr., P. Muller, and P. C. Gallacher, 1985: Wind direction and equilibrium mixed layer depth in the tropical Pacific Ocean. *J. Phys. Oceanogr.*, **15**, 1332-1338.
- Gregg, M. C., H. Peters, J. C. Wesson, N. S. Oakey, and T. J. Shay, 1985: Intensive measurements of turbulence and shear in the equatorial undercurrent. *Nature*, **318**, 140-144.
- Moum, J. N., and D. R. Caldwell, 1989: Mixing in the equatorial surface layer. *J. Geophys. Res.*, **94**, 2005-2021.
- Moum, J. N., D. R. Caldwell, C. A. Paulson, T. K. Chereskin, and L. A. Regier, 1986: Does ocean turbulence peak at the equator? *J. Phys. Oceanogr.*, **16**, 1991-1994.
- Muller, P., 1976: On the diffusion of momentum and mass by internal gravity waves. *J. Fluid Mech.*, **77**, 789-823.
- Muller, P., and R. W. Garwood, Jr., 1988: Mixed layer dynamics: Progress and new directions. *EOS*, **69**, 2-12.
- Muller, P., R. W. Garwood, Jr., and J. P. Garner, 1984: Effect of vertical advection on the dynamics of the oceanic surface mixed layer. *Annales Geophys.*, **2**, 387-398.
- Obukhov, A. M., 1946: Turbulence in an atmosphere with a nonuniform temperature. *Trudy Inst. Teoret. Geofiz. AN SSSR*, **1**; translated and reprinted in *Bound.-Layer Meteor.*, **2**, 1971.
- Hughes, R. L., 1980: On the equatorial mixed layer. *Deep-Sea Res.*, **27A**, 1067-1078.
- Paka, V. T., and K. N. Fedorov, 1982: Influence of the thermal structure of the upper ocean layer on the development of turbulence. *Izvest., Atmos. Ocean Phys.*, **18**, 134-138.
- Peters, H., M. C. Gregg, and J. M. Toole, 1988: On the parameterization of equatorial turbulence. *J. Geophys. Res.*, **93**, 1199-1218.
- Rossby, C. G., and R. B. Montgomery, 1935: The layer of frictional influence in wind and ocean currents. *Pap. Phys. Oceanogr. Meteor.*, **3**, 101 pp.
- Schopf, P. S., and M. A. Cane, 1983: On equatorial dynamics, mixed layer physics and sea surface temperature. *J. Phys. Oceanogr.*, **13**, 917-935.
- Weare, B. C., P. T. Strub, and M. D. Samuel, 1981: Annual mean surface heat fluxes in the tropical Pacific Ocean. *J. Phys. Oceanogr.*, **11**, 705-717.
- Wyrtki, K., 1981: An estimate of equatorial upwelling in the Pacific. *J. Phys. Oceanogr.*, **11**, 1205-1214.
- Wyrtki, K., and G. Meyers, 1976: The trade wind field over the Pacific Ocean. *J. Appl. Meteor.*, **15**, 694-704.

**WESTERN PACIFIC INTERNATIONAL MEETING
AND WORKSHOP ON TOGA COARE**

Nouméa, New Caledonia

May 24-30, 1989

PROCEEDINGS

edited by

Joël Picaut *

Roger Lukas **

Thierry Delcroix *

* ORSTOM, Nouméa, New Caledonia

** JIMAR, University of Hawaii, U.S.A.

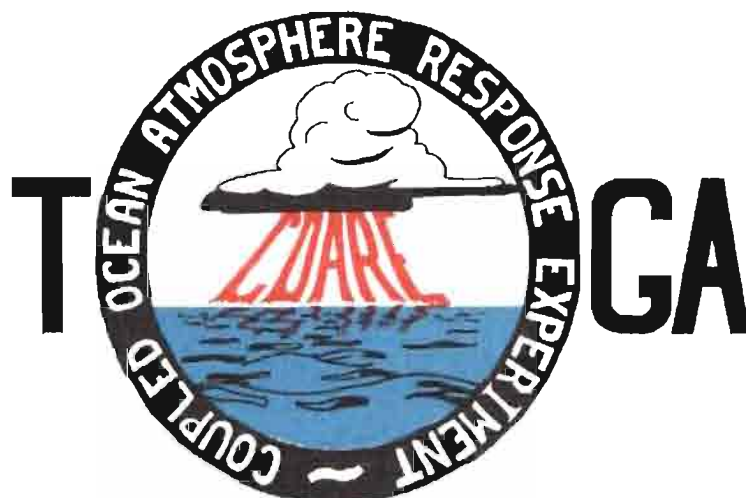


TABLE OF CONTENTS

ABSTRACT	i
RESUME	iii
ACKNOWLEDGMENTS	vi
INTRODUCTION	
1. Motivation	1
2. Structure	2
LIST OF PARTICIPANTS	5
AGENDA	7
WORKSHOP REPORT	
1. Introduction	19
2. Working group discussions, recommendations, and plans	20
a. Air-Sea Fluxes and Boundary Layer Processes	20
b. Regional Scale Atmospheric Circulation and Waves	24
c. Regional Scale Oceanic Circulation and Waves	30
3. Related programs	35
a. NASA Ocean Processes and Satellite Missions	35
b. Tropical Rainfall Measuring Mission	37
c. Typhoon Motion Program	39
d. World Ocean Circulation Experiment	39
4. Presentations on related technology	40
5. National reports	40
6. Meeting of the International Ad Hoc Committee on TOGA COARE	40
APPENDIX: WORKSHOP RELATED PAPERS	
Robert A. Weller and David S. Hosom: Improved Meteorological Measurements from Buoys and Ships for the World Ocean Circulation Experiment	45
Peter H. Hildebrand: Flux Measurement using Aircraft and Radars	57
Walter F. Dabberdt, Hale Cole, K. Gage, W. Ecklund and W.L. Smith: Determination of Boundary-Layer Fluxes with an Integrated Sounding System	81

MEETING COLLECTED PAPERS

WATER MASSES, SEA SURFACE TOPOGRAPHY, AND CIRCULATION

Klaus Wyrtki: Some Thoughts about the West Pacific Warm Pool	99
Jean René Donguy, Gary Meyers, and Eric Lindstrom: Comparison of the Results of two West Pacific Oceanographic Expeditions FOC (1971) and WEPOCS (1985-86)	111
Dunxin Hu, and Maochang Cui: The Western Boundary Current in the Far Western Pacific Ocean	123
Peter Hacker, Eric Firing, Roger Lukas, Philipp L. Richardson, and Curtis A. Collins: Observations of the Low-latitude Western Boundary Circulation in the Pacific during WEPOCS III	135
Stephen P. Murray, John Kindle, Dharma Arief, and Harley Hurlburt: Comparison of Observations and Numerical Model Results in the Indonesian Throughflow Region	145
Christian Henin: Thermohaline Structure Variability along 165°E in the Western Tropical Pacific Ocean (January 1984 - January 1989)	155
David J. Webb, and Brian A. King: Preliminary Results from Charles Darwin Cruise 34A in the Western Equatorial Pacific	165
Warren B. White, Nicholas Graham, and Chang-Kou Tai: Reflection of Annual Rossby Waves at The Maritime Western Boundary of the Tropical Pacific	173
William S. Kessler: Observations of Long Rossby Waves in the Northern Tropical Pacific	185
Eric Firing, and Jiang Songnian: Variable Currents in the Western Pacific Measured During the US/PRC Bilateral Air-Sea Interaction Program and WEPOCS	205
John S. Godfrey, and A. Weaver: Why are there Such Strong Steric Height Gradients off Western Australia ?	215
John M. Toole, R.C. Millard, Z. Wang, and S. Pu: Observations of the Pacific North Equatorial Current Bifurcation at the Philippine Coast	223

EL NINO/SOUTHERN OSCILLATION 1986-87

Gary Meyers, Rick Bailey, Eric Lindstrom, and Helen Phillips: Air/Sea Interaction in the Western Tropical Pacific Ocean during 1982/83 and 1986/87	229
Laury Miller, and Robert Cheney: GEOSAT Observations of Sea Level in the Tropical Pacific and Indian Oceans during the 1986-87 El Nino Event	247
Thierry Delcroix, Gérard Eldin, and Joël Picaut: GEOSAT Sea Level Anomalies in the Western Equatorial Pacific during the 1986-87 El Nino, Elucidated as Equatorial Kelvin and Rossby Waves	259
Gérard Eldin, and Thierry Delcroix: Vertical Thermal Structure Variability along 165°E during the 1986-87 ENSO Event	269
Michael J. McPhaden: On the Relationship between Winds and Upper Ocean Temperature Variability in the Western Equatorial Pacific	283

John S. Godfrey, K. Ridgway, Gary Meyers, and Rick Bailey: Sea Level and Thermal Response to the 1986-87 ENSO Event in the Far Western Pacific	291
Joël Picaut, Bruno Camusat, Thierry Delcroix, Michael J. McPhaden, and Antonio J. Busalacchi: Surface Equatorial Flow Anomalies in the Pacific Ocean during the 1986-87 ENSO using GEOSAT Altimeter Data	301

THEORETICAL AND MODELING STUDIES OF ENSO AND RELATED PROCESSES

Julian P. McCreary, Jr.: An Overview of Coupled Ocean-Atmosphere Models of El Nino and the Southern Oscillation	313
Kensuke Takeuchi: On Warm Rossby Waves and their Relations to ENSO Events	329
Yves du Penhoat, and Mark A. Cane: Effect of Low Latitude Western Boundary Gaps on the Reflection of Equatorial Motions	335
Harley Hurlburt, John Kindle, E. Joseph Metzger, and Alan Wallcraft: Results from a Global Ocean Model in the Western Tropical Pacific	343
John C. Kindle, Harley E. Hurlburt, and E. Joseph Metzger: On the Seasonal and Interannual Variability of the Pacific to Indian Ocean Throughflow	355
Antonio J. Busalacchi, Michael J. McPhaden, Joël Picaut, and Scott Springer: Uncertainties in Tropical Pacific Ocean Simulations: The Seasonal and Interannual Sea Level Response to Three Analyses of the Surface Wind Field	367
Stephen E. Zebiak: Intraseasonal Variability - A Critical Component of ENSO ?	379
Akimasa Sumi: Behavior of Convective Activity over the "Jovian-type" Aqua-Planet Experiments	389
Ka-Ming Lau: Dynamics of Multi-Scale Interactions Relevant to ENSO	397
Pecheng C. Chu and Roland W. Garwood, Jr.: Hydrological Effects on the Air-Ocean Coupled System	407
Sam F. Iacobellis, and Richard C.J. Somerville: A one Dimensional Coupled Air-Sea Model for Diagnostic Studies during TOGA-COARE	419
Allan J. Clarke: On the Reflection and Transmission of Low Frequency Energy at the Irregular Western Pacific Ocean Boundary - a Preliminary Report	423
Roland W. Garwood, Jr., Pecheng C. Chu, Peter Muller, and Niklas Schneider: Equatorial Entrainment Zone : the Diurnal Cycle	435
Peter R. Gent: A New Ocean GCM for Tropical Ocean and ENSO Studies	445
Wasito Hadi, and Nuraini: The Steady State Response of Indonesian Sea to a Steady Wind Field	451
Pedro Ripa: Instability Conditions and Energetics in the Equatorial Pacific	457
Lewis M. Rothstein: Mixed Layer Modelling in the Western Equatorial Pacific Ocean	465
Neville R. Smith: An Oceanic Subsurface Thermal Analysis Scheme with Objective Quality Control	475
Duane E. Stevens, Qi Hu, Graeme Stephens, and David Randall: The hydrological Cycle of the Intraseasonal Oscillation	485
Peter J. Webster, Hai-Ru Chang, and Chidong Zhang: Transmission Characteristics of the Dynamic Response to Episodic Forcing in the Warm Pool Regions of the Tropical Oceans	493

MOMENTUM, HEAT, AND MOISTURE FLUXES BETWEEN ATMOSPHERE AND OCEAN

W. Timothy Liu: An Overview of Bulk Parametrization and Remote Sensing of Latent Heat Flux in the Tropical Ocean	513
E. Frank Bradley, Peter A. Coppin, and John S. Godfrey: Measurements of Heat and Moisture Fluxes from the Western Tropical Pacific Ocean	523
Richard W. Reynolds, and Ants Leetmaa: Evaluation of NMC's Operational Surface Fluxes in the Tropical Pacific	535
Stanley P. Hayes, Michael J. McPhaden, John M. Wallace, and Joël Picaut: The Influence of Sea-Surface Temperature on Surface Wind in the Equatorial Pacific Ocean	543
T.D. Keenan, and Richard E. Carbone: A Preliminary Morphology of Precipitation Systems In Tropical Northern Australia	549
Phillip A. Arkin: Estimation of Large-Scale Oceanic Rainfall for TOGA	561
Catherine Gautier, and Robert Frouin: Surface Radiation Processes in the Tropical Pacific	571
Thierry Delcroix, and Christian Henin: Mechanisms of Subsurface Thermal Structure and Sea Surface Thermo-Haline Variabilities in the South Western Tropical Pacific during 1979-85 - A Preliminary Report	581
Greg. J. Holland, T.D. Keenan, and M.J. Manton: Observations from the Maritime Continent : Darwin, Australia	591
Roger Lukas: Observations of Air-Sea Interactions in the Western Pacific Warm Pool during WEPOCS	599
M. Nunez, and K. Michael: Satellite Derivation of Ocean-Atmosphere Heat Fluxes in a Tropical Environment	611

EMPIRICAL STUDIES OF ENSO AND SHORT-TERM CLIMATE VARIABILITY

Klaus M. Weickmann: Convection and Circulation Anomalies over the Oceanic Warm Pool during 1981-1982	623
Claire Perigaud: Instability Waves in the Tropical Pacific Observed with GEOSAT	637
Ryuichi Kawamura: Intraseasonal and Interannual Modes of Atmosphere-Ocean System Over the Tropical Western Pacific	649
David Gutzler, and Tamara M. Wood: Observed Structure of Convective Anomalies	659
Siri Jodha Khalsa: Remote Sensing of Atmospheric Thermodynamics in the Tropics	665
Bingrong Xu: Some Features of the Western Tropical Pacific: Surface Wind Field and its Influence on the Upper Ocean Thermal Structure	677
Bret A. Mullan: Influence of Southern Oscillation on New Zealand Weather	687
Kenneth S. Gage, Ben Basley, Warner Ecklund, D.A. Carter, and John R. McAfee: Wind Profiler Related Research in the Tropical Pacific	699
John Joseph Bates: Signature of a West Wind Convective Event in SSM/I Data	711
David S. Gutzler: Seasonal and Interannual Variability of the Madden-Julian Oscillation	723
Marie-Hélène Radenac: Fine Structure Variability in the Equatorial Western Pacific Ocean	735
George C. Reid, Kenneth S. Gage, and John R. McAfee: The Climatology of the Western Tropical Pacific: Analysis of the Radiosonde Data Base	741

Chung-Hsiung Sui, and Ka-Ming Lau: Multi-Scale Processes in the Equatorial Western Pacific	747
Stephen E. Zebiak: Diagnostic Studies of Pacific Surface Winds	757

MISCELLANEOUS

Rick J. Bailey, Helene E. Phillips, and Gary Meyers: Relevance to TOGA of Systematic XBT Errors	775
Jean Blanchot, Robert Le Borgne, Aubert Le Bouteiller, and Martine Rodier: ENSO Events and Consequences on Nutrient, Planktonic Biomass, and Production in the Western Tropical Pacific Ocean	785
Yves Dandonneau: Abnormal Bloom of Phytoplankton around 10°N in the Western Pacific during the 1982-83 ENSO	791
Cécile Dupouy: Sea Surface Chlorophyll Concentration in the South Western Tropical Pacific, as seen from NIMBUS Coastal Zone Color Scanner from 1979 to 1984 (New Caledonia and Vanuatu)	803
Michael Szabados, and Darren Wright: Field Evaluation of Real-Time XBT Systems	811
Pierre Rual: For a Better XBT Bathy-Message: Onboard Quality Control, plus a New Data Reduction Method	823